

#1341

ASSIMILATING LANDSAT IMAGERY IN A GRASSLAND GROWTH MODEL: A CASE STUDY IN ARIZONA

Moran, M.S., Y. Nouvellon, R.B. Bryant and W. Ni
U.S. Water Conservation Laboratory
4331 E. Broadway Rd.
Phoenix, Arizona 85719
moran@tucson.ars.ag.gov

ABSTRACT

This study presents a modeling approach to combine a soil-vegetation-atmosphere transfer (SVAT) model with Landsat imagery to produce images of spatially-distributed living plant and root biomass. The model was run for a 10-year period with 25 Landsat Thematic Mapper (TM) images over a USDA watershed (~150 km²) in Arizona for grassland-dominated regions. This manuscript addresses the special issues associated with applying the approach on a spatially-distributed basis, including minimizing computer run time, processing TM images for atmospheric and other "unwanted" noise, and obtaining spatially-distributed meteorological conditions for model input. The results from this work will provide a blueprint for similar studies with other models and images at other locations.

INTRODUCTION

Assimilation of remote sensing in plant and soil process models combines the spatial coverage of the imagery with the greater temporal frequency of the model outputs to provide accurate, distributed information about plant and soil conditions on a daily or hourly basis. Though there are a multitude of robust, validated process models and there are numerous orbiting sensors providing calibrated, multi-spectral data, merging these two technologies is not trivial. Assimilation is generally achieved by an iterative model "calibration" procedure using the intermittent spectral information to estimate several model parameters and/or initial conditions, thus increasing the model accuracy. Once such an approach has been developed and validated at one site, the next step is to apply the model in a spatially-distributed manner at a local or regional scale with satellite-based imagery. To do so, there are several issues that must be addressed, including:

- Accounting for differences in model, image and process temporal and spatial scales;
- Minimizing computer time required for model runs and the iterative calibration;
- Processing images to account for atmospheric and other unwanted "noise"; and
- Obtaining spatially-distributed meteorological conditions.

These issues were addressed in a case study in Arizona in which a soil-vegetation-atmosphere-transfer (SVAT) model for perennial grasslands was combined with Landsat 5 Thematic Mapper (TM) and Landsat 7 Enhanced TM Plus (ETM+) images to provide daily maps of plant biomass, green leaf area index, soil moisture and sensible and latent heat fluxes over a ten-year period 1990-1999. Though the combined remote sensing/modeling approach had been validated at a test site with ground-based inputs, this was our first attempt to apply the model in a spatially-distributed manner with satellite-based images. The following sections will address the methods used to minimize computing time, correct images for atmospheric effects, and obtain spatially-distributed information on meteorological conditions. The manuscript will conclude with a short presentation of modeling results and model validation with ground-based measurements of plant biomass. More detailed information on modeling results is presented in a companion paper by Nouvellon et al. (2000).

APPROACH

The combined remote sensing/modeling approach used here is based on the assumption that the SVAT model is capable of realistically simulating the temporal evolution of useful surface variables, but that the simulations are inaccurate due to the lack of information on some important model input parameters or initial conditions. Since the SVAT model can simulate the canopy structural variables required by a canopy reflectance model, reflectance

measurements can then be used to constrain the simulations of the model and, through an iterative procedure, facilitate optimal selection of the unknown model input parameters or initial conditions (Nouvellon et al., 1999b). This approach is illustrated graphically in Figure 1.

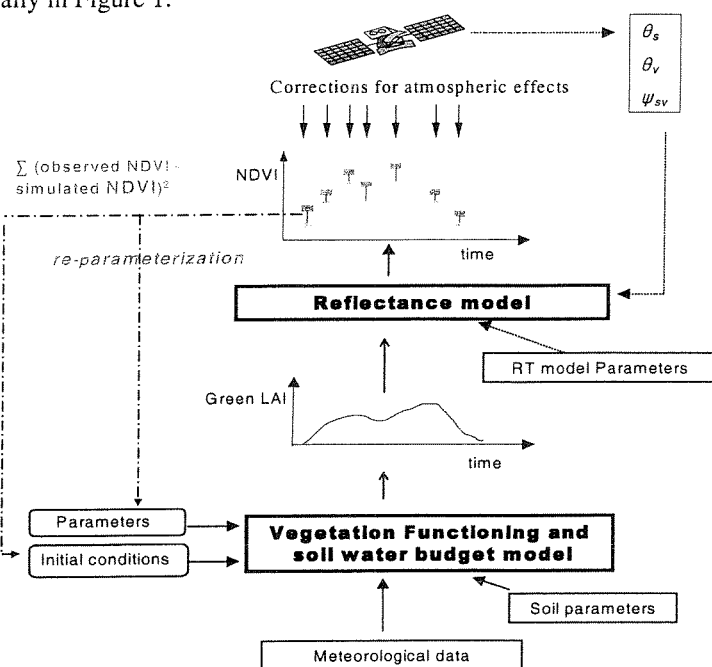


Figure 1. A graphic illustration of the combined remote sensing/modeling approach with the iterative re-initialization/re-parameterization procedure used to improve model accuracy with Landsat spectral data.

Models

The SVAT model used in this study consists of two submodels designed to simulate plant growth and water budget (Figure 2). The plant growth submodel is driven by standard daily meteorological data and simulates daily biomass dynamics of green shoots, dead shoots and living root biomass. The water budget submodel simulates plant transpiration, evaporation from bare soil, and soil water fluxes. This model has been validated with measurements of actual evapotranspiration measurements, soil moisture, plant biomass and leaf area index acquired on several short-grass ecosystems in southeast Arizona, USA and northeast Sonora, Mexico (Nouvellon et al., 1999a).

In this methodology, a canopy radiative transfer model (RTM) was linked with the plant growth model through the simulated green leaf area index (GLAI). The Markov Chain of Canopy Reflectance (MCCR) RTM was selected for this study (Kuusk, 1995). A comparison of MCCR-simulated and measured reflectances was used to assess the ability of the model to produce reasonable estimates of near-infrared (NIR) and red canopy reflectances (ρ_{NIR} and ρ_{Red} , respectively). An iterative procedure was used to minimize the difference between simulated and measured NDVI by changing values of selected model initial conditions or input parameters. NDVI is the normalized difference vegetation index, where $\text{NDVI} = (\rho_{\text{NIR}} - \rho_{\text{Red}}) / (\rho_{\text{NIR}} + \rho_{\text{Red}})$ and is highly sensitive to the amount of green, photosynthesizing vegetation.

Parameters and initial conditions chosen to be re-parameterized/re-initialized were such that (1) the model was highly sensitive to them, (2) they were spatially variable, and (3) they were difficult to obtain by direct measurements at a regional scale. Following a sensitivity analysis, and taking into account these three criteria, initial living root biomass (BR_{ini}) and maximum light use efficiency (ϵ_{qmax}) of absorbed photosynthetically active radiation (APAR) were selected to be initialized and parameterized, respectively. An interactive procedure based on the downhill simplex method (Nelder and Mead, 1965) was used to estimate the values of ϵ_{qmax} and BR_{ini} that minimized the difference between simulated and measured NDVI.

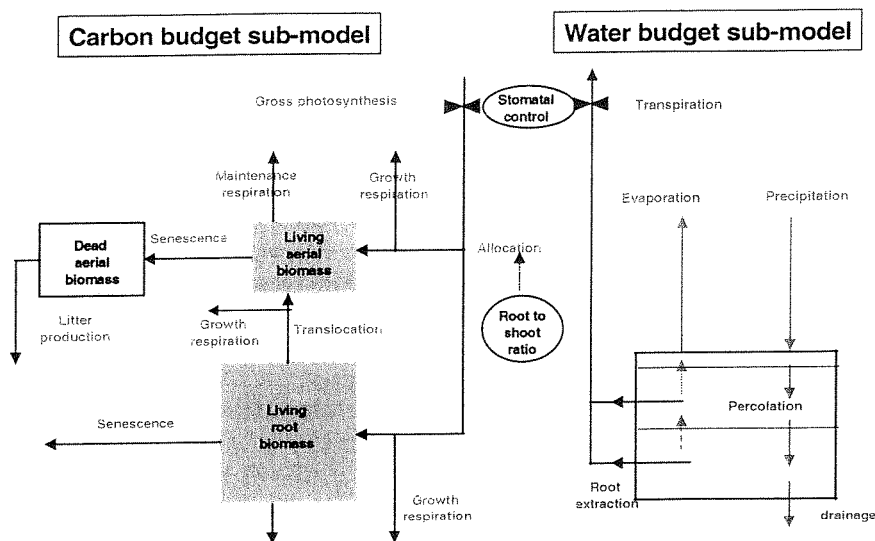


Figure 2. The general flow of the soil-vegetation-atmosphere-transfer (SVAT) model with the carbon budget and water budget sub-models.

Experiment

A spatially-distributed application of the combined remote sensing/SVAT approach was attempted at the local scale (~150 km²) with Landsat TM images (30 m ground resolution) over a 10-year period (from 1990-1999). The test site for this study was the USDA-ARS Walnut Gulch Experimental Watershed (WGEW: 31°43'N; 100°W) within the Upper San Pedro Basin (USPB) in southeastern Arizona. Elevation within the watershed ranges from about 1300 m above mean sea level (MSL) to about 1800 m MSL 20 km to the east. The grassland vegetation in WGEW is dominated by perennial C4 grasses, where the dominant species are black grama (*Bouteloua eriopoda*), curly mesquite (*Hilaria belangeri*), hairy grama (*Bouteloua hirsuta*) and three awn (*Aristida hamulosa*). In this region, precipitation ranges from 250 to 500 mm/yr, with two thirds of the rainfall occurring during the summer “monsoon season” in July and August.

Meteorological data for the model were acquired by instrumentation located in the Kendall watershed, near the east end of WGEW (Figure 3a). There were few gaps in this 10-year set of daily meteorological measurements, and these gaps were filled with measurements made with identical instrumentation several kilometers to the west, but still within WGEW. Information on precipitation amount and timing was taken from a rain gage located near the meteorological station at Kendall. To accomplish the ten-year run of the model, we obtained all the Landsat TM images available within this ten-year period during the grassland growing season (basically, July-October) with clear-sky conditions. This resulted in an accumulation of 29 images acquired by the Landsat-5 TM and Landsat-7 ETM+ sensors from 1990 to 1999 (Table 1). Landsat 7 ETM+ images were ordered but were not received and processed at the time of this writing (descriptions of the Landsat 5 TM and Landsat 7 ETM+ sensors is included in Table 2).

To validate some of the components of this approach, it was necessary to measure surface reflectance of large targets in the TM spectral bands using the following methodology. Reflectance (ρ) was measured with 4-band Exotech radiometers with TM filters and the 8-band Modular Multispectral Radiometer (MMR) simulating all 7 TM spectral bands. The reference reflectance standard was a 2' by 2' BaSO₄ or molded halon plate that was calibrated frequently for absolute reflectance and non-lambertian properties (Jackson et al., 1987). For ground-based measurements, the Exotech or MMR radiometers were mounted in backpack-like yokes that held the sensor in a nadir-looking position about 2 m above the surface and 1 m from the right shoulder of the operator. Thus, the operator made a multitude of measurements along designated transects, and returned to make frequent measurements of the reference plate. During most Landsat overpasses at WGEW, we made yoke-based measurements of ρ over a 480 m by 120 m (16 by 4 TM pixels) target of uniform vegetation within the Kendall sub-watershed. Measurements of this large, uniform target were generally completed within 20 minutes.

Landsat5 TM Images 1990	8/24/90	9/9/90	10/11/90	
Landsat5 TM Images 1991	9/4/91	10/14/91		
Landsat5 TM Images 1992	9/30/92			
Landsat5 TM Images 1993	7/31/93	8/16/93	9/1/93	9/17/93
Landsat5 TM Images 1994	10/22/94			
Landsat5 TM Images 1995	8/6/95	8/22/95	9/23/95	10/9/95
Landsat5 TM Images 1996	7/7/96	7/23/96	8/24/96	
Landsat5 TM Images 1997	8/27/97	9/28/97	10/14/97	
Landsat5 TM Images 1998	7/29/98	8/14/98	8/30/98	10/1/98
Landsat7 ETM+ Images 1999	7/24/99	8/25/99	9/10/99	9/26/99

	Landsat-5 TM	Landsat-7 ETM+
Spectral Band Central Wavelengths (μm)	TM1: 0.486; TM2: 0.570; TM3: 0.660; TM4: 0.840; TM5: 1.676; TM7: 2.223; TM6: 11 (same as ETM+)	
Spatial Resolution	30 m MS; 120 m TIR	30 m MS; 60 m TIR; 15 m Pan

To measure the bidirectional reflectance factor as a function of sensor viewing angle (θ_v), an Exotech radiometer was mounted on a 2 m swinging boom that allowed ρ of a target of approximately 0.5 m diameter to be measured over the range of $-45^\circ < \theta_v < 45^\circ$ at 5° increments. Results from these measurements were used to determine the surface bidirectional reflectance distribution function (BRDF) through simulation models for bare soils and plant canopies (Qi et al., 1995). The general approach was to use the yoke-based measurements over a large target for an assessment of the absolute ρ , and use the boom-based device to determine the shape of the relation between ρ and θ_v (Jackson et al., 1990).

MINIMIZING COMPUTER TIME REQUIRED FOR MODEL RUNS

The SVAT model described in the previous section was run on a personal computer (PC) in the MATLAB environment with C- and Fortran-based submodels, and a threshold of 50 iterations per model calibration. With this configuration, it took approximately 3 minutes to run the model for one set of surface conditions over the 10-year period of interest. At 30 m resolution, there would be 60,199 model runs to cover the entire grassland region in WGEW (Figure 3a). As a result, it would take over 125 days to run one model simulation for every grassland pixel in WGEW. Certainly, with further refinement to the code and transfer to a more powerful computer system, the model run time could be decreased; but even if the model run time were reduced to five seconds, it would still take over 3.5 days to complete the model run for the 10-year period. Excessive computer time is a common issue in temporal model applications to large regions, particularly when an iterative calibration procedure is involved.

To minimize the time consumed by model runs, we reduced the redundancy of surface conditions by classifying the 60,199 pixels into 25 "similar" classes based on NDVI (Figure 3b). NDVI was chosen for classification since it was the variable passed between the SVAT model and the canopy RTM for model calibration. An unsupervised classification of the TM-derived NDVI from the 25 TM images resulted in 25 distinct classes related to similar temporal NDVI "signatures". This reduced the number of required model runs to 25 (classes) per each of 24 soil types (Figure 3c), or

600 possible combinations. For our experimental site, the total number of different soil and spectral class combinations was only 374, resulting in 374 model runs at 3 minutes per run for a total time of less than 19 hours. For a ten-year period at a daily time step, this computational time requirement was considered reasonable.

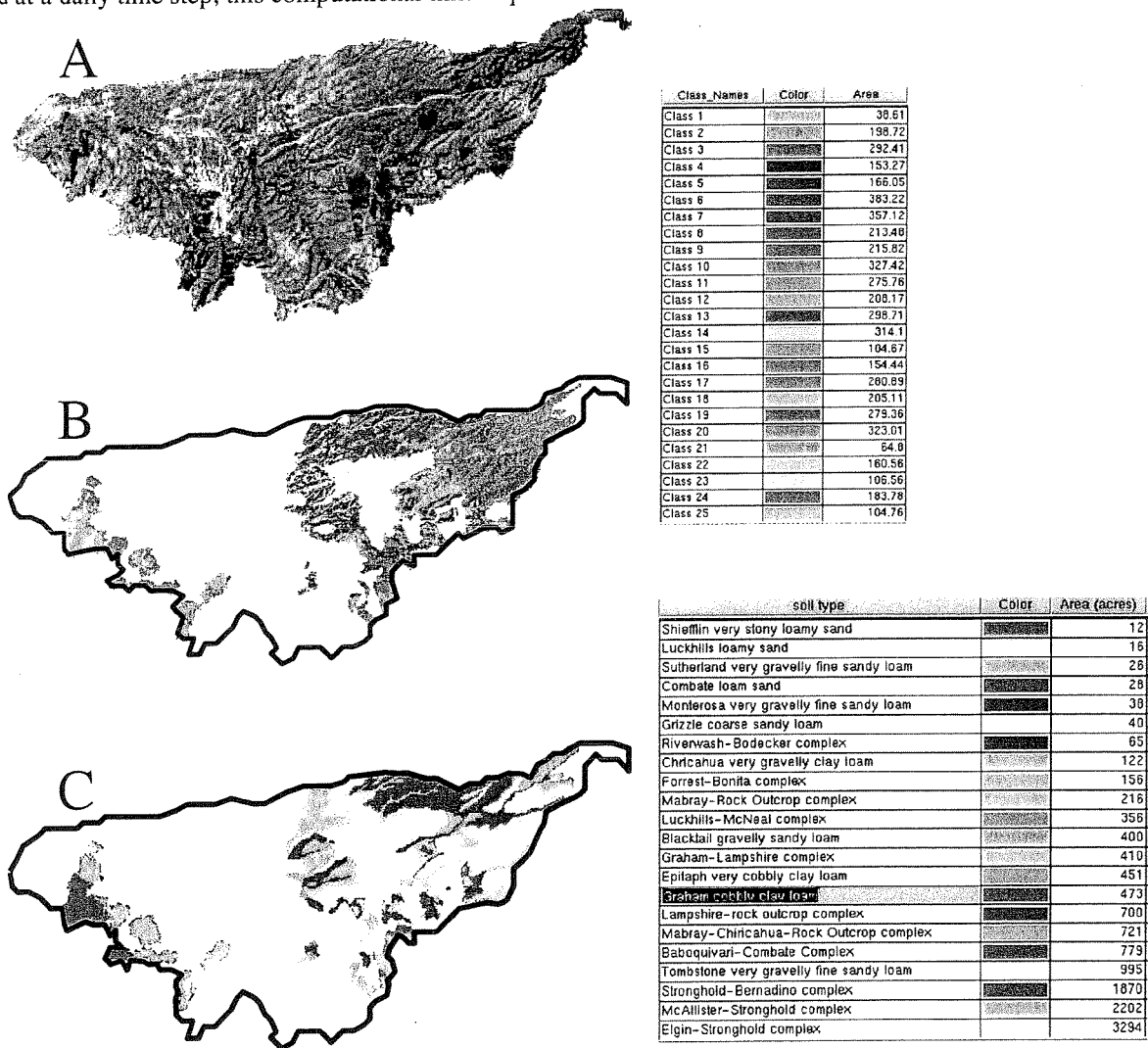


Figure 3. Images of the Walnut Gulch Experimental Watershed (WGEW), where image (a) is a Landsat-5 TM color composite of the entire watershed (27 Aug 1997), and images (b) and (c) have been filtered to show only the grassland-dominated regions. Image (b) is the result of an unsupervised classification of NDVI from all the Landsat-5 TM images from 1990-1999, and image (c) is a map of soil types.

PROCESSING IMAGES TO ACCOUNT FOR ATMOSPHERE AND OTHER NOISE

For model application, it was necessary to convert image data from a raw digital number (*dn*) to surface reflectance to minimize effects of sensor, solar and atmospheric variations. This was accomplished by defining a linear relation between image *dn* and surface reflectance based on a target of known reflectance within the image and an estimate of the *dn* associated with zero reflectance, as described in the following subsections.

Pseudo-Invariant Objects

Since atmospheric conditions were unknown for the majority of the images, it was necessary to find a correction approach based on an existing target within all scenes of known spectral reflectance (often termed a "pseudo-invariant

object” or PIO). By our definition, a PIO is a target with a strong, known, invariant relation between the spectral surface reflectance (ρ) and the solar zenith and sensor view angles (θ_z and θ_v , respectively). The required time period of “invariance” is dependent upon the application; that is, a target could qualify as a PIO even if the surface degrades slowly over time (e.g., a painted target) or changes abruptly at a known time (e.g., a surface with occasional resurfacing) as long as the relation between ρ , θ_z , and θ_v is periodically recharacterized. Thus, for any date and time, the reflectance of the PIO is known and can be used to determine a dn -to-reflectance ratio to retrieve surface reflectance factors from image dn .

For WGEW, we identified two PIO: a packed earth airplane parking lot (100 by 100 m) associated with a local landing strip, and an area of bright mine tailings covering an area of approximately 400 by 400 m. We made surface reflectance measurements at both sites using yoke- and boom-based radiometers to derive the relation between ρ and θ_z . Yoke-based measurements of ρ were made for the packed earth parking lot with a nadir-looking sensor from dawn to solar noon on five dates in 1998. Boom-based measurements of ρ were made at sensor viewing angles (θ_v) from -45° to $+45^\circ$ at two θ_z for the same target. A BRDF model (Shibayama and Wiegand, 1985) was inverted using measured surface bidirectional reflectances, so that parameters were available to determine parking lot ρ and values of θ_v and θ_s (Figure 4). Similarly, we found a strong relation between θ_s and ρ for a flat area of approximately 200 by 200 m within the bright mine tailings at WGEW (Figure 5). The mine PIO was preferable for this modeling work because it met the size required for Landsat-type sensors (i.e., 5 by 5 pixels or 0.15 by 0.15 km).

To investigate the effect that precipitation might have on this PIO, we sprinkled the surface of the packed earth parking lot and the mine with enough water to saturate the surface to a depth of 2 cm. Measurements made before and after saturation showed that for summer conditions at $\sim 10:00$ MST with cloud-free conditions and moderate winds, ρ decreased substantially with increased soil moisture but returned to the pre-application ρ within 15-20 minutes (Figure 6). Considering that images for this work were acquired with cloud-free conditions, the effects of precipitation on the characterized PIO would be minimal.

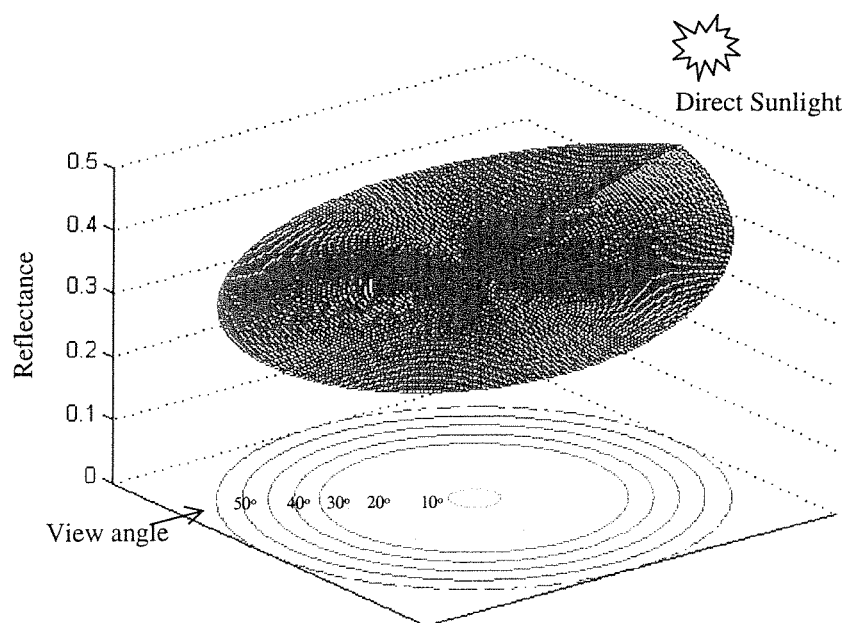


Figure 4. The bidirectional reflectance distribution function (BRDF) of a packed-earth parking lot at WGEW in the principal plane of the sun with solar zenith angle 45° .

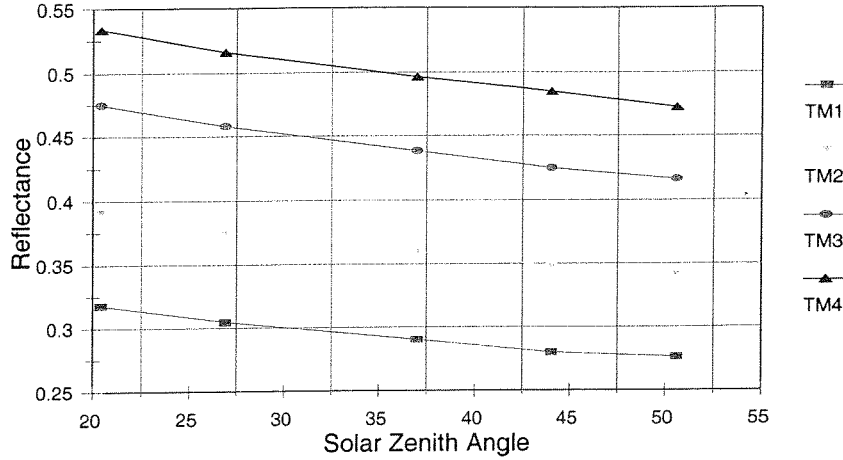


Figure 5. The relation between solar zenith angle (θ_z) and surface reflectance (ρ) in the first four TM spectral bands for a bright mine tailing at WGEW ($\theta_v=0^\circ$).

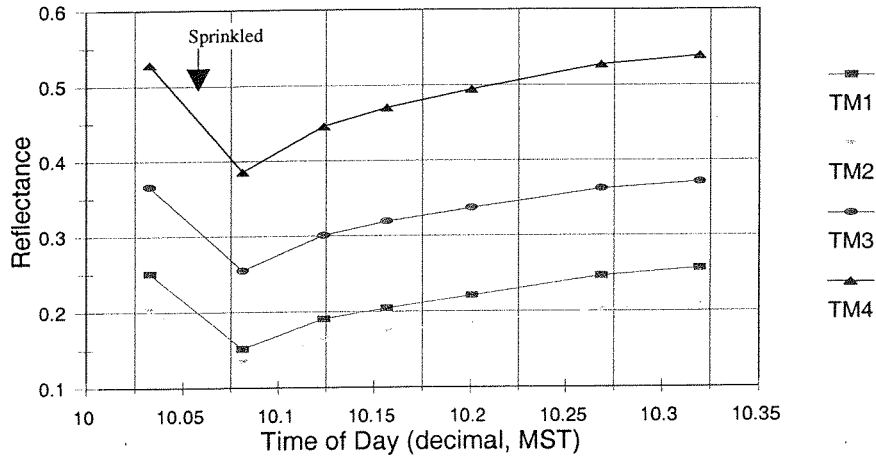


Figure 6. Temporal measurements of surface reflectance (ρ) of the WGEW mine surface with dry, wet and drying conditions.

Reflectance Factor Retrieval and Accuracy Assessment

Based on these results, we retrieved surface reflectance from the dn of 25 TM images (Table 1) using a linear relation between surface reflectance and image dn determined by two points. The first point was simply the reflectance of the mine at the time and date of the TM overpass, computed from the relation between mine ρ and θ_s and θ_v as modeled with the SOILSPECT model (Jacquemond et al., 1992) calibrated using the mine ground-based reflectance measurements (Figure 5). The second point was the digital number associated with zero reflectance as determined for typical atmospheric conditions in SE Arizona on cloud-free days. The latter was determined based on historical measurements of surface reflectance of multiple sites in Arizona with associated TM dn . A linear relation was determined between measurements of surface reflectance and TM dn , and this relation was extrapolated to determine the TM dn associated with zero reflectance, where dn for zero reflectances was determined to be 16.3, 15.5 and 9.1 for TM bands 2-4, respectively (Moran et al., 1995). Alternatively, this determination could have been made simply by running an atmospheric radiative transfer model for zero surface reflectance with standard atmospheres suitable for this region.

This atmospheric correction procedure based on the estimated mine reflectance and the dn associated with zero reflectance was employed to correct all 25 TM images used in this project. The results of this correction were validated by comparison of TM-retrieved reflectances with yoke-based measurements of reflectance at a large grassland target (120 by 480 m) in Kendall on four dates within the 10-year period: 10 Sep 1990, 4 Sep 1991, 1 Oct 1992 and 20 Mar 1997 (Figure 7). This independent validation of the atmospheric correction procedure showed that the root mean squared (RMS) error of retrieved reflectance was less than 0.01. This level of accuracy is equal to that obtained using conventional in-flight calibration techniques (Slater et al, 1987) and met the accuracy requirements for the modeling project. These results confirmed the invariance of the PIO and validated our estimate of the dn associated with a zero reflectance target.

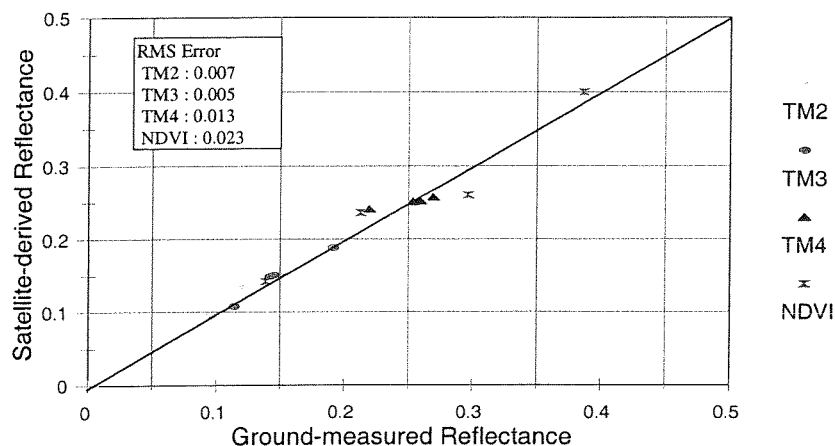


Figure 7. Comparison of ground-based reflectances with reflectance derived from Landsat5 TM digital number (dn) using the atmospheric correction procedure based on the pseudo-invariant object procedure.

OBTAINING SPATIALLY-DISTRIBUTED METEOROLOGICAL INFORMATION

One of the greatest difficulties in taking a model from a point-based to a spatially-distributed application is the determination of spatially-distributed meteorological information such as air temperature (T_a) and wind speed (U). This is particularly difficult because T_a and U are highly variable with changes in surface topography and land cover, and most SVAT models are very sensitive to small errors in T_a and U . We are currently testing an approach to retrieve spatially-distributed meteorological data at a fine 4- km resolution from a mesoscale meteorological model.

The Regional Atmospheric Modeling System (RAMS) is a mesoscale meteorological model designed to predict the variability in surface atmospheric forcing arising from heterogeneous land cover and complex topography (Pielke et al., 1992). RAMS has the potential to be run in near real-time to provide spatially-distributed, local-scale information about moisture, temperature and wind fields consistent with the underlying surface. For this application, the RAMS model needed basic boundary conditions at a coarse resolution, and spatially-distributed information about surface characteristics at a finer resolution. In a study conducted by Toth (1997), the RAMS model was run in near real-time with basic boundary conditions estimated by approximately 30- km mesoscale "Eta" data produced by the National Weather Service's National Center for Environmental Prediction (NCEP). Local-scale information about surface characteristics was incorporated into the model using a two-way coupling of Landsat Thematic Mapper (TM) data with RAMS. The result was the generation of images of local-scale forcing variables at 4- km resolution over the semi-arid San Pedro River Basin (USPB: 230 by 230 km) in southeast Arizona.

Several changes to the standard RAMS surface scheme were required, as outlined in more detail by Toth (1997). To account for the hot, dry conditions in USPB, the model was refined to allow for differences in roughness lengths for heat and momentum in the computation of sensible heat flux. Another change was the inclusion of a computation of surface skin temperature, based on a gradient between the upper and next-to-upper soil layers (both 0.75 cm thick), to allow comparison of RAMS-estimated surface skin temperature and TM-measured skin temperature. A third change was in determination of soil thermal conductivity (a function of the soil moisture potential in RAMS) to account for the rapid increase in conductivity for soils of very low soil moisture (as found in the semi-arid Southwest). A fourth change was

to the vegetation categories and associated parameters, where the standard biosphere-atmosphere transfer scheme (BATS) categories were replaced with a locally-defined set of ten land categories (1:agriculture, 2:sage-oak, 3:grassland, 4:conifer, 5:oak-grass, 6:sage-creosote, 7:creosote-mesquite, 8:sage-grass, 9:alpine, and 10:playa) and the fraction cover of vegetation, albedo, roughness lengths, and leaf area index for each category were refined based on the Landsat TM values of NDVI for this region. A final change was to refine the parameterization of the stomatal conductance function (which determines the latent heat flux between vegetation and air) based on the use of remotely-sensed measurements of surface skin temperature to improve estimates of stomatal conductance.

This refined RAMS model (termed here RAMS') was run in near real-time mode in 1997 producing fields of forcing variables at 4-km resolution for USPB at 6-hour intervals. Examples of the RAMS' fields of air temperature, wind speed, water vapor mixing ratio, and precipitable water are included in Figure 8 for 9 June 1997. Though the accuracy of these fields has not been validated, the link to underlying surface conditions is apparent when RAMS' outputs were compared with spatially-distributed information about vegetation type and surface elevation for the same region (Figure 9). From visual analysis, it also appears that RAMS' outputs are comparable to fields of T_a and an improvement over fields of U produced by interpolating between measurements from ground-based meteorological stations (Figure 10). Differences in clarity of images in Figures 8, 9 and 10 are due largely to the spatial resolution, where Figure 8 images have 4-km resolution and images in Figure 9 and 10 have 100-m resolution.

The RAMS'-derived meteorological fields illustrated here were not used for this modeling run for three reasons: 1) the RAMS' fields were not yet validated; 2) this run covers only a local region (150 km^2), and 3) the RAMS' fields were only available for one year (1997) of this ten-year study. These RAMS' fields will provide spatially distributed meteorological conditions for a second SVAT run over a larger region for a one-year period.

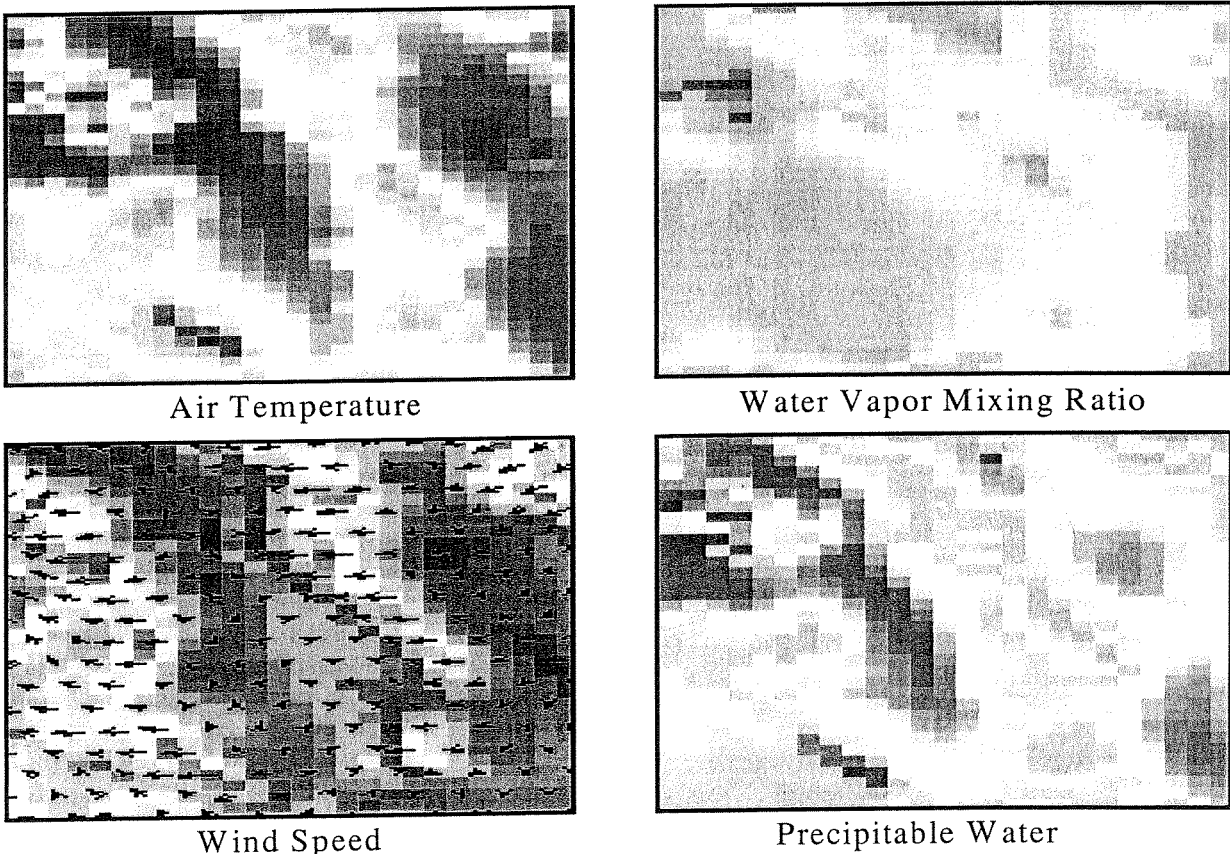
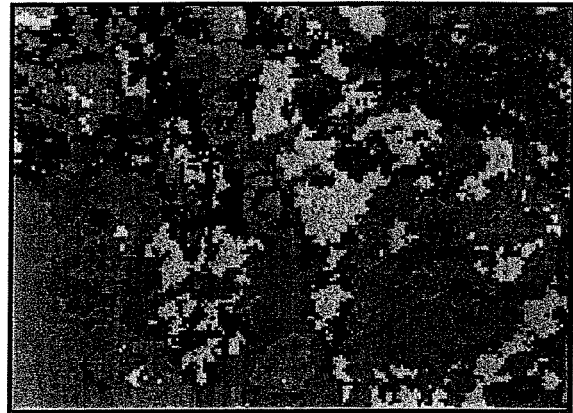


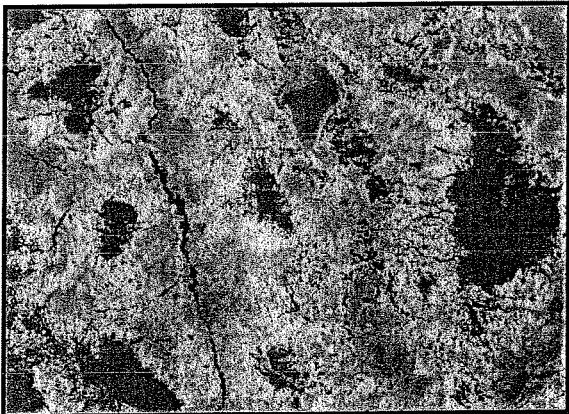
Figure 8. Fields of a) air temperature, b) wind speed, c) water vapor mixing ratio, and d) precipitable water at 4-km resolution over a region of 100 by 100 km, derived from near real-time runs of the refined Regional Atmospheric Modeling System (RAMS') for the Upper San Pedro Basin on 9 June 1997. North is at the top, the scale is approximately one inch to 40 km, and the longitude and latitude of the upper left and lower right corners are $110^{\circ}39' \text{ N}$, $32^{\circ}26' \text{ E}$ and $109^{\circ}08' \text{ N}$ and $31^{\circ}27' \text{ E}$, respectively.



Surface Temperature



Vegetation Biome



Spectral Vegetation Index

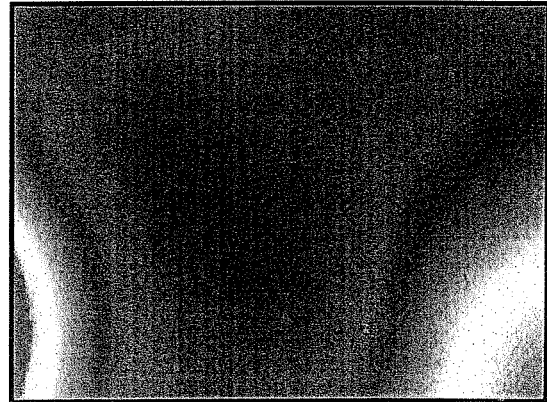


Surface Elevation

Figure 9. Images of surface temperature and reflectance (color composite) measured by the Landsat5 TM sensor on 17 June 1997 (left) and images of vegetation biomes (upper right; 10 classes listed in text) and surface elevation (lower right; from 800 to 3000 *km*) for the same region in Figure 8 at 100 *m* resolution.



Air Temperature



Wind Speed

Figure 10. Images of air temperature and wind speed at height 2 *m* produced by interpolation of data measured at 15 stations within Upper San Pedro Basin (USPB). The air temperature image was interpolated using a technique to account for surface elevation; the wind speed image was simply interpolated without regard to topography, for the same region as Figure 8 at 100 *m* resolution on 17 June 1997 (Moran et al., 1996).

MODEL RESULTS

The SVAT model was run for a ten year period from 1990 to 1999 for the grassland region in WGEW based on meteorological data from the Kendall sub-watershed, a map of soil types (Figure 3c), and spectral data from 25 Landsat5 TM images (Table 1). At the Kendall site, the model calibration (based on comparison of remotely-sensed and modeled estimates of NDVI) resulted in estimates of BR_{ini} and ϵ_{qmax} of 323 g/m^2 and $7.59 \text{ g dry matter MJ}^{-1} \text{ APAR}$, respectively. The daily simulations of plant biomass for the ten-year period for the Kendall site are presented as solid lines in Figure 11. The difference between modeled and measured plant biomass (solid circles in Figure 11) for years 1990-1992 resulted in a RSME of only 11.7 g/m^2 . In contrast, when the model was run with an a-priori set of possible values of BR_{ini} and ϵ_{qmax} based on published literature (Charles-Edwards et al., 1986; $BR_{ini}=300 \text{ g/m}^2$ and $\epsilon_{qmax}=6.2 \text{ g dry matter MJ}^{-1} \text{ APAR}$), the RMSE was nearly double at 19.3 g/m^2 (Figure 11). The results presented here for Kendall show the potential for using this remote sensing/modeling approach to produce an accurate map of above-ground biomass for the entire WGEW for any day during the ten-year period. Further validation at another location based on measurements made in summer 1999 (not yet processed) will provide greater confidence in the methodology. Details on model design, parameterization, calibration and results for the entire WGEW grassland are included in a companion paper by Nouvellon et al. (2000).

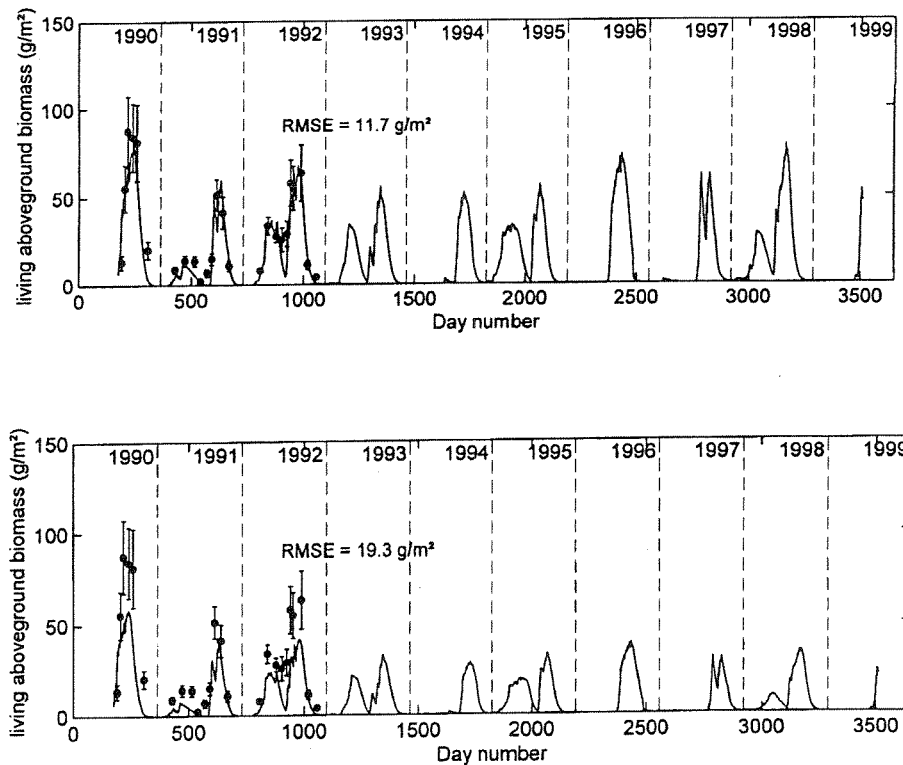


Figure 11. Daily simulations of plant above-ground biomass at the Kendall site for the period 1990-1999 based on the combined remote sensing/modeling approach to re-parameterize and re-initialize the model (upper figure) and based on the model alone with reasonable estimates of BR_{ini} and ϵ_{qmax} (lower figure).

CONCLUDING REMARKS

This report presents a successful application of a remote sensing/modeling approach for mapping grassland above-ground and root biomass at the local scale over a 10-year period. Data showed that the model calibration with Landsat TM images resulted in greatly improved estimates of aboveground green biomass at the Kendall grassland site. The application of the model at the local scale also resulted in new approaches for minimizing computer run time, processing

TM images for atmospheric and other "unwanted" noise, and obtaining spatially-distributed meteorological conditions for model input. The latter approaches will be useful all temporal applications of SVAT models at other locations.

Our next step will be to incorporate the Landsat7 ETM+ images that had been ordered for the year 1999, but had not been received at the time of this writing (Table 1). During each Landsat-7 overpass, we made measurements of surface reflectance at Kendall, measurements of atmospheric optical depth using a sun photometer, and weekly measurements of plant biomass throughout WGEW. With these measurements, we will be able to confirm the in-flight calibration of the ETM+ sensor, determine the ETM+ dn associated with zero reflectance with a standard WGEW atmosphere, and provide further validation of the 10-year modeling results using 1999 measurements of plant biomass.

ACKNOWLEDGMENTS

This work was funded by NASA Landsat7 Science Team (NASA S-41396-F). Work on the RAMS model was funded by the Electric Power Research Institute (EPRI). We are indebted to Dr. Kuusk for providing the MCCR model and to the staff of the USDA Southwest Watershed Research Center (SWRC) and WGEW for support and data.

REFERENCES

- Charles-Edwards, D.A., D. Doley and G.M. Rimmington (1986) Modeling plant growth and development, Academic Press, Orlando, Fla.
- Jackson, R.D., M.S. Moran, P.N. Slater and S.F. Biggar (1987) Field calibration of reference reflectance panels, Rem. Sens. Environ. 22:145-158.
- Jackson, R.D., P.M. Teillet, P.N. Slater, G. Fedosejevs, M.F. Jasinski, J.K. Aase and M.S. Moran (1990) Bidirectional measurements of surface reflectance for view angle corrections of oblique imagery, Rem. Sens. Environ. 32:189-202.
- Jacquemond, S., F. Baret and J.F. Hanocq (1992) Modeling spectral and bidirectional soil reflectance, Rem. Sens. Environ. 41:123-132.
- Kuusk, A. (1995) A Markov chain model of canopy reflectance, Agr. For. Meteorol. 76:221-236.
- Moran, M.S., R.D. Jackson, T.R. Clarke, J. Qi, F. Cabot, K.J. Thome and B.N. Markham (1995) Reflectance factor retrieval from Landsat TM and SPOT HRV data for bright and dark targets, Rem. Sens. Env. 52:218-230.
- Moran, M.S., A.F. Rahman, J.C. Washburne, D.C. Goodrich, M.A. Weltz and W.P. Kustas (1996) Combining the Penman-Monteith equation with measurements of surface temperature and reflectance to estimate evaporation rates of semiarid grassland, Agric. For. Meteorol. 80:87-109.
- Nelder, J.A. and R. Mead (1965) A simplex method for function minimization, Comput. J. 7:308-313.
- Nouvellon, Y., D. LoSeen, S. Rambal, A. Begue, M.S. Moran, Y. Kerr and J. Qi (1999a) Time course of radiation use efficiency in a shortgrass ecosystem: consequences for remotely-sensed estimation of primary production, Rem. Sens. Env. (in press).
- Nouvellon, Y.P., M.S. Moran, R.B. Bryant, W. Ni, P. Hielman, D. LoSeen, A. Bégéu, S. Rambal and J. Qi (2000) Combining a SVAT model with Landsat imagery for a ten year simulation of grassland carbon and water budget, 2nd Intl. Geospat. Inform. in Agric. and Forestry Conf., 10-23 January 2000, Lake Buena Vista, Fla. (In press).
- Nouvellon, Y., S. Rambal, D. LoSeen, M.S. Moran, J.P. Lhomme, A. Begue, A.G. Chehbouni and Y. Kerr (1999b) A process-based model for daily fluxes of water and carbon in shortgrass ecosystem, J. Agr. For. Met. (in press).
- Pielke, R.A., W.R. Cotton, R.L. Walko, C.J. Tremback, W.A. Lyons, L.D. Grasso, M.E. Nicholls, M.D. Moran, D.A. Wesley, T.J. Lee and J.H. Copeland (1992) A comprehensive meteorological modeling system - RAMS, Meteor. Atmos. Phys. 49:69-91.
- Qi, J., M.S. Moran, F. Cabot and G. Dedieu, (1995) Normalization of sun/view angle effects on vegetation indices with bidirectional reflectance function models, Rem. Sens. Env. 52:207-217.
- Shibayama, M. and C.L. Wiegand (1985) View azimuth and zenith, and solar angle effects using spectral albedo-based vegetation indices, Rem. Sens. Environ. 18:91-103.
- Slater, P.N., S.F. Biggar, R.G. Holm, R.D. Jackson, Y. Mao, M.S. Moran, J.M. Palmer and B. Yuan (1987) Reflectance- and radiance-based methods for the in-flight absolute calibration of multispectral sensors, Rem. Sens. Environ. 22:11-37.
- Toth, J.J. (1997) Coupling Landsat data with a mesoscale model to estimate evapotranspiration, AMS 13th Conf. on Hydrology 2-7 February, Long Beach, Cal., P9.6.